


RESEARCH

Open Access



# Long-term therapeutic effects of allogeneic mesenchymal stem cell transplantation for intrauterine adhesions

Kai Chen<sup>1†</sup>, Yanyan Gao<sup>2†</sup>, Ninuo Xia<sup>3,4</sup>, Yusheng Liu<sup>2</sup>, Huiru Wang<sup>1</sup>, Hui Ma<sup>3</sup>, Shengxia Zheng<sup>1,3\*</sup> and Fang Fang<sup>3\*</sup> 

## Abstract

**Background** Intrauterine adhesion (IUA), resulting from uterine trauma, is one of the major causes of female infertility. Previous studies have demonstrated that endometrial mesenchymal stem cells (eMSC) have therapeutic effects on IUA through cellular secretions. It is particularly true for most of the pre-clinical experiments performed on multiple animal models, as human-derived eMSC cannot maintain long-term engraftment in animals. Whether tissue-specific MSCs from allogeneic origin can engraft and exert long-term therapeutic efficacy has yet to be thoroughly explored.

**Methods** We established a rat IUA model to study the long-term engraftment and therapeutic effects of eMSC derived from humans and rats. Human and rat eMSC were isolated and verified by the expression of cell surface markers and the ability to differentiate into osteoblasts, adipocytes, and chondrocytes. The cells were then labeled by green fluorescence proteins (GFP) and transplanted to the rat uterus *ex vivo* and *in vivo*. The engraftment was investigated by the expression of GFP at different days after transplantation. Assessed the therapeutic effects by examining the endometrial thickness, the number of glands, and the pregnancy outcome. Significantly, we conducted a thorough assessment of the local cellular immune response following both xenograft and allograft transplantation.

**Results** H-eMSC were eliminated by rats' immune systems within three days after transplantation. In contrast, R-eMSC successfully engrafted and persisted in rat tissue for over ten days. Notably, R-eMSC significantly improved the pregnancy rate by enhancing endometrial thickness and increasing the number of glands, while also reducing fibrosis in rat IUA models. Additionally, the immune response to R-eMSC was generally less aggressive compared to that of xenogeneic MSCs.

**Conclusions** Tissue-specific MSCs from the allogeneic origin can integrate into the repaired tissue and exert long-term therapeutic efficacy in the model of IUA. This study indicates that in addition to secreting therapeutic factors short-time, tissue-specific MSCs may engraft and participate in long-time tissue repair and regeneration.

**Keywords** Intrauterine adhesion, Endometrial mesenchymal stem cells, Stem cell therapy, Animal model

<sup>†</sup>Kai Chen and Yanyan Gao have contributed equally to this work and should be considered co-first authors.

\*Correspondence:

Shengxia Zheng  
zhengshengxia@ustc.edu.cn  
Fang Fang  
fangfang0724@gmail.com

Full list of author information is available at the end of the article



## Introduction

The normal endometrium plays a vital role in establishing and maintaining pregnancy [1]. Curettage after abortion and postpartum hemorrhage will damage the endometrial tissue and form intrauterine adhesion (IUA) [2, 3]. IUA is one of the leading causes of infertility [4]. It causes embryo implantation failure, miscarriages, and abnormal placentation during late pregnancy [4–6]. Current clinical treatment for IUA includes hysteroscopic adhesion lysis, hormonal manipulation, and vasoactive therapies [7–9]. However, most treatments are only applicable or practical to patients with mild or moderate IUA [10]. Novel strategies to treat severe IUA have become a major challenge in the field.

With the rapid development of stem cell biology, stem cell transplantation has been considered a promising treatment for IUA, especially for patients with severe IUA [11–14]. An increasing number of researchers have focused on the application of mesenchymal stem cells (MSCs) [15]. MSCs are multipotent cells that can be derived from several tissues, such as adipose tissue, bone marrow, and endometrial tissue [12, 16, 17]. MSCs attract intensive attention for cell-based therapy due to their unique characteristics, including differentiation ability, paracrine activity, and immunomodulatory effects [18]. Thus, MSCs have been applied in treating a variety of diseases, including brain diseases, heart diseases, and reproductive diseases [19–21].

MSCs from different sources have been studied in IUA, such as bone marrow-derived MSCs, adipose-derived MSCs, and umbilical cord-derived MSCs. Interestingly, the application of endometrial mesenchymal stem cells (eMSC) has been gained a lot of attention recently and rapidly growing [22]. This is mainly due to the high homology of eMSC with uterine tissue and their potential for autologous treatment. Although several animal studies have shown that transplantation of human-derived MSCs can promote endometrial regeneration of animals [23], the therapeutic effects are considered short-term, as the immune system rapidly clears human cells from the animals [24]. The mechanism for these xenotransplantation assays is mostly the paracrine activity of the stem cells. Whether tissue-specific MSCs of allogeneic or autogenic origin can engraft and exert long-term therapeutic efficacy has not been thoroughly explored.

In this study, we aim to examine the engraftment and the retention time of human- and rat-derived eMSC in the rat uterus. We will explore the underlying molecular mechanisms and evaluate the therapeutic effects of allogeneic eMSC transplantation in a rat IUA model.

## Materials and methods

### Animals

Eight- to ten-week-old Sprague Dawley female rats weighing 180–220 g were used in all experiments, and all rats were purchased from Shanghai SLAC Laboratory Animals. The rats had free access to water and food and were maintained in a feeding room on a 12 h light and 12 h dark regimen with an average temperature of 22 °C and 70% to 80% relative humidity. All the procedures were approved by the Institutional Animal Care and Use Committee at the First Affiliated Hospital of USTC (code no. 2022-N(A)–119). The work has been reported in line with the ARRIVE guidelines 2.0.

### Collection of human endometrium and rat endometrium samples

Human endometrial samples were obtained from nonmenopausal women who underwent hysteroscopy for nonneoplastic disease from the Department of Obstetrics and Gynecology. All donors gave consent, and all procedures were approved by the Ethics Committee of First Affiliated Hospital of USTC (IRB code NO. 2023KY300). Patients are required to be free of hormone use for the previous 3 months before surgery. Endometrium samples were collected into Dulbecco's modified Eagle's medium (DMEM, BI, CAT#:01–051–1ACS) supplemented with 100 U/ml penicillin, 100 µg/mL streptomycin (Biosharp, CAT#: BL505A), and 10% fetal bovine serum (FBS, Sigma, CAT#: F7524). When removed from the human endometrium, it will be better treated within 6 h.

It has been reported that MSCs isolated from aged rats have a low proliferation and differentiation capacity [25]. Therefore, rat endometrial samples were obtained from 8- to 10-week-old Sprague Dawley female rats weighing 180–220 g. In brief, the rats were killed, and the uterus was removed immediately. The rat uterus was transferred into the culture medium and then used for cell isolation.

### Isolation of endometrial mesenchymal stem cells (eMSC)

Human endometrial tissue and rat endometrial tissue were treated using the same method. First, the tissue was cut into 1 mm × 1 mm pieces and washed with phosphate-buffered saline (PBS, CAT#: BI, 02–024–1ACS) 2 times to completely remove the culture medium. Second, the tissue pieces were transferred to a 15 ml Falcon tube containing 1 ml enzyme mix: 0.4 ml collagenase IV (10 mg/mL, CAT#: Gibco, 17,104–019), 0.4 ml collagenase V (10 mg/mL, CAT#: Solarbio, C8170), 0.2 mL DNase I (1 mg/mL, CAT: Biofrox, 1121MG010) and 3 ml PBS. Then, the tube was placed in a shaker at 37 °C for 40 min. At the end of digestion, the mixture was centrifuged at 800 revolutions per minute (RPM) for 5 min. The supernatant was discarded and mixed with red cell

lysis solution (CAT#: Biosharp, BL503B) to destroy red blood cells. Finally, the mixture was dissolved in PBS and screened through a 70  $\mu\text{m}$  sieve at 800 RPM for 5 min to centrifuge the mixture through the sieve. The pellet was resuspended in DMEM containing 10% FBS, 1% penicillin and streptomycin and cultured at 37 °C in a 5% CO<sub>2</sub> atmosphere, with a medium change every 2–3 days.

#### Flow cytometry analysis

After 3 passages, cells were digested from the culture dish with Accutase, resuspended in FACS buffer, and counted. For H-eMSC, flow cytometry analysis was conducted using a Human MSC Analysis Kit (CAT#: BD Biosciences, 562,245) based on the manufacturer's protocol. For rat endometrium-derived mesenchymal stem cells (R-eMSC). An SD rat MSC Analysis Kit (CAT#: Cyagen, RAXMX-0901) was used for cell surface marker identification. All results were analyzed using FlowJo, version 10, software.

#### Differentiation of H-eMSC and R-eMSC into adipocytes, osteocytes, and chondrocytes

To identify the ability of human endometrium-derived mesenchymal stem cells (H-eMSC) to differentiate into multiple mesenchymal lineages (adipogenic, osteogenic, and chondrogenic). We used a Human MSC Functional Identification kit (CAT #: R&D Systems, SC006) based on the manufacturer's protocol. Finally, we employed oil red O, alizarin red, and toluidine blue staining to verify the successful differentiation of mesenchymal stem cells into adipocytes, osteoblasts, and chondrocytes.

To induce R-eMSC differentiation into adipocytes and osteocytes. We used the Adipogenic Differentiation Induction Kit (CAT#: Cyagen, RAXMX-90031) and Osteogenic Differentiation Induction Kit (CAT#: Cyagen, RAXMX-90021) according to the manufacturer's instructions. Briefly, after 3 weeks of differentiation, adipocytes, osteocytes, and chondrocytes were identified by staining with oil red O, alizarin red, and toluidine blue, respectively.

#### Determining the estrus period of rats

We used vaginal secretions from rats to determine whether they were in the estrus phase as previously described [26]. Briefly, a cotton swab dipped in normal saline was inserted into the vagina of a rat. The swab was scratched gently inside the vagina to obtain the cells. The cotton was gently rubbed across a slide to collect the cells, and then the cell composition was observed under a microscope. A large number of cornified epithelial cells showed that the rats were in the estrus phase.

#### Establishment of the rat intrauterine adhesion (IUA) model

Rats in estrus were selected based on vaginal smear analysis and anesthetized with Zoletil 50 (Virbac France) (0.1 ml/100 g) by muscle injection. The lower abdomen was disinfected with iodophor after shaving, and then the skin and muscle were cut across the midline to expose the uterus. A 3–5 mm longitudinal incision was made in the uterus, and tweezers were inserted into the uterus of the rats and rubbed 20 times in all directions. The uterine surface was washed with 10 ml saline, and the uterine horn was closed using absorbable sutures. A total of about 60 female rats were used in this experiment. All rats were randomly assigned to each group.

#### GFP labeling of cells

We labeled H-eMSC and R-eMSC with an rAAV vector expressing GFP (Tsingke, China). A total of  $1 \times 10^6$  cells (P3) were incubated in 1  $\mu\text{l}$  rAAV working solution at 37 °C for up to 1 day, washed with PBS, and cultured in fresh medium containing 10% FBS. After 4 days, GFP expression was analyzed using a fluorescence microscope.

#### Transplantation of H-eMSC and R-eMSC ex vivo

A female rat was sacrificed (stopped breathing after a cervical dislocation), and its uterus was removed and cut along the long axis of the rat uterus using surgical scissors. The endometrium was scratched with a surgical blade 20 times, and the uterus was washed using PBS. A total of  $2 \times 10^6$  cells labeled with GFP were transferred to the surface of the rat endometrium. Some medium was added to the culture dish and cultured at 37 °C in a 5% CO<sub>2</sub> atmosphere. Subsequently, the tissues were taken at different time points for direct observation and frozen sectioning. All ex vivo transplantation experiments were conducted at least three times.

#### Frozen section

The rat uterus (3–4 mm) was placed in a small sealed box, and OCT was performed (CAT: # biosharp, BL557A). The sealed box was frozen in liquid nitrogen for 10–20 s. Equilibrate at –20 °C for approximately 15 min to prevent cracking of the tissue block when sectioning. Section the block at a range of 10–15  $\mu\text{m}$  and place it on adhesive slides. Finally, the slides were observed directly under a fluorescence microscope.

#### Immunofluorescence

First, the paraffin sections were deparaffinized using xylene and then subjected to antigen retrieval.

Following the repair, the sections were sealed at room temperature for one hour before being incubated with antibodies (CD45, CAT#: Abcam, ab10558, USA. CD68, CAT#: CST, 97778S, USA) overnight. The next day, the sections were incubated with secondary antibodies (Jackson labs, USA) at room temperature, shielded from light, for one hour. The nuclei were subsequently stained with DAPI (CAT#: Biosharp, BS097, China) and observed and counted using a fluorescence microscope (ZESIS). All immunofluorescence experiments were conducted at least three times for reliability.

### Transplantation of H-eMSC and R-eMSC in vivo

The rats were divided into 3 groups. One group was transplanted with GFP-labeled H-eMSC, one group was transplanted with H-GFP-eMSC and immunosuppressed with methotrexate (H-eMSC+MTX) (CAT#: T1485, TargetMol, USA) and the last group was transplanted with R- GFP-eMSC. The left uterus of the rat was used for IUA modeling, and the right was used for IUA + eMSC therapy. GFP-labeled cells ( $2 \times 10^6$  cells dissolved in 20  $\mu$ l DMEM) were injected into the left uterus of each rat, and the same volume of DMEM was injected into the right uterus as a control.

### In vivo fluorescence imaging

Cardiac perfusion with normal saline was performed after the rats were anesthetized, and the uterus was subjected to imaging with an in vivo imaging system (Perkin Elmer, IVIS Spectrum, USA). The images were obtained at 1 d, 3 d, and 10 d after transplantation.

### Flow cytometry to identify GFP-expressing cells

After the uterus was removed, the endometrial tissue of rats was digested according to a previously described cell isolation method. Two groups of single-cell suspensions were obtained by digesting each side uterus of rats. Single cells were dissolved in FSCS buffer before analysis. Then, IUA modeling was used as a negative control, and IUA + eMSC therapy was used as the experimental group.

### Hematoxylin and eosin (H&E) and MASSON staining

After the rat uterus was removed from the rat, paraformaldehyde was fixed at room temperature for at least 1 day and then embedded in paraffin. The sections were cut into 5–10  $\mu$ m thick continuous sections. The HE and MASSON staining were used to assess the intimal thickness, number of glands, and degree of fibrosis consistent with previous methods [14]. Endometrial thickness was measured from the luminal epithelium to the smooth muscle layer with imaging. The average of the measurement results of two mutually perpendicular lines is taken.

### Fertility test

Eight- to ten-week-old Sprague Dawley female rats weighing 180–220 g were used in the cell therapy experiment. Group 1 (3VS3) was the sham operation group on the left and the control (without any treatment). In group 2, the left uterus was the sham-operated side, and the right side was the IUA side (15VS15). In group 3, the left uterus was the sham-operated side, and the right side was the IUA + R-eMSC therapy side (15VS15). In group 4, the left uterus was the sham-operated side, and the right side was the IUA + auto-eMSC therapy side (15VS15). On the 10th day after treatment, the female rats were housed together with healthy male rats at a ratio of 2:1. Discovery of the female rat vaginal plug was considered day 0 of pregnancy. The pregnant rats were sacrificed on gestation days 14–18, and the number of embryos on both sides was counted.

### Statistical analysis

Statistical analysis was performed using GraphPad Prism 7 (San Diego, CA, USA). Quantitative data are represented as the mean  $\pm$  standard deviation obtained from a minimum of three independent experiments. Statistical significance was determined by Student's t-test or one-way analysis of variance, and  $*P < 0.05$ ,  $**P < 0.01$ ,  $***P < 0.001$ , and  $****P < 0.0001$  were considered to indicate a statistically significant difference.

(See figure on next page.)

**Fig. 1** Isolate MSCs from human and rat endometria and identification. **(A)** Schematic diagram of H-eMSC and R-eMSC isolated from rat and human endometrium. **(B)** Bright-field morphology of H-eMSC. Scale bar: 200  $\mu$ m **(C)** Bright field morphology of R-eMSC. Scale bar: 200  $\mu$ m **(D)** Isolated human endometrium single cells at passage 4 were used for flow cytometry analyses, and the values represent the percentage of positive cells among all accessed cells. **(E)** Oil red O, alizarin red, and toluidine blue staining to verify the successful differentiation of H-eMSC into adipocytes, osteoblasts, and chondrocytes. Adipogenesis Scale bar: 50  $\mu$ m, Osteogenesis and Chondrogenesis Scale bar: 200  $\mu$ m. **(F)** Isolated rat endometrium single cells at passage 3 were used for flow cytometry analyses, and the values represent the percentage of positive cells among all accessed cells. **(G)** Oil red O, alizarin red, and toluidine blue staining to verify the successful differentiation of R-eMSC into adipocytes, osteoblasts, and chondrocytes. Scale bar: 200  $\mu$ m. (n = 3)

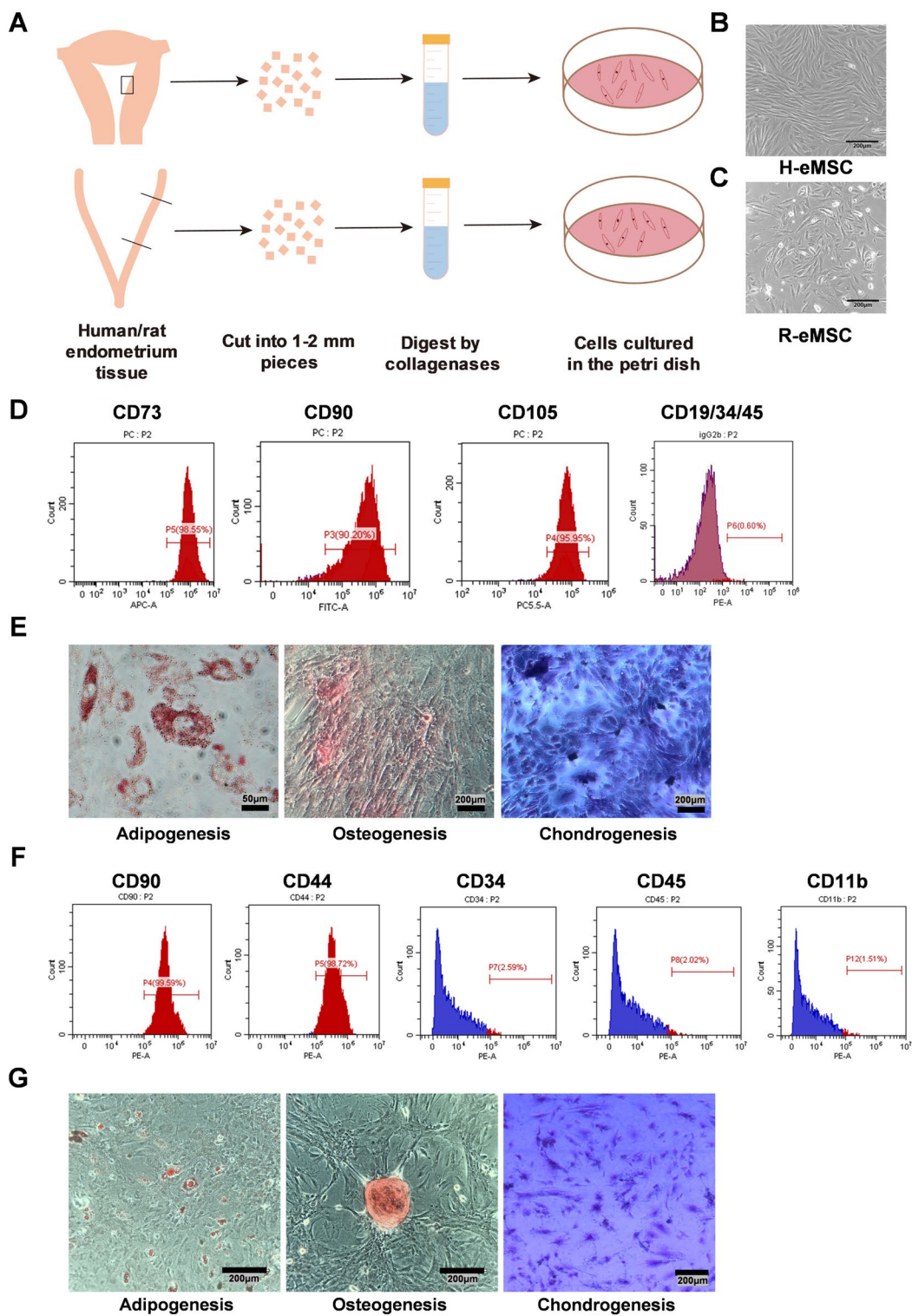


**Fig. 1** (See legend on previous page.)

**Results**

**Isolation and characterization of H-eMSC and R-eMSC**

We isolated eMSC from human and rat endometrial

tissue respectively (Fig. 1A). H-eMSC exhibited a uniform fibroblast-like spindle morphology and tended to align in bundles (Fig. 1B). R-eMSC displayed a similar

fibroblast-like morphology, but they were shorter with irregular alignment (Fig. 1C). Both cell types demonstrated great proliferative ability at passage 3 (P3). Cells after P3 were used for all the following experiments to get rid of the other cell types in the primary culture.

To characterize the immunophenotype of the cells, we performed flow cytometry analysis to examine cell surface marker proteins of H-eMSC at P3. As shown in Fig. 1D, more than 90% of the H-eMSC were positive for MSC markers (CD90, CD73, and CD105), and less than 1% of the H-eMSC were positive for other cell surface markers, such as CD11b, CD19, CD34, CD45 and HLA-DR. To determine the multipotent differentiation of H-eMSC, we cultured cells at P3 in osteogenic, adipogenic, and chondrogenic differentiation-inducing culture medium. After 14–21 days of differentiation, we utilized oil red O, alizarin red, and toluidine blue staining to confirm the successful differentiation of H-eMSC into adipocytes, osteoblasts, and chondrocytes (Fig. 1E).

Similarly, we characterized the properties of R-eMSC. R-eMSC were strongly positive for CD44 and CD73 and negative for CD34, CD45, and CD11b (Fig. 1F). Oil red O, alizarin red, and toluidine blue staining confirm the successful differentiation of R-eMSC into adipocytes, osteoblasts, and chondrocytes (Fig. 1G). Together, we successfully isolated eMSC from human and rat uteri and characterized the immunophenotype and differentiation potential of the cells.

#### Transplantation of MSCs ex vivo

To investigate whether transplanted eMSC can adhere to the endometrial tissue, we performed the transplantation ex vivo. We labeled H-eMSC and R-eMSC with GFP and transplanted them onto the surface of the rat uterus (Fig. 2A). Then, we monitored the transplanted GFP<sup>+</sup> cells under a fluorescence microscope at 1 h, 12 h, 3 d, and 10 d, respectively. As shown in Fig. 2B and C, the cell morphology changed from spherical to polygonal 12 h after transplantation (Fig. 2) B and C, indicating that R-eMSC and H-eMSC have attached to the rat endometrium at this time. Importantly, these GFP<sup>+</sup> cells were engrafted and survived for more than 10 days after transplantation. In addition to fluorescence microscopy, we further confirmed the engraftment by frozen sections. Collectively, these results show that H-eMSC and R-eMSC can adhere to the rat endometrium and be retained for long-term ex vivo.

#### Transplantation of MSCs in vivo

We went on to investigate whether H-eMSC and R-eMSC can engraft and persist in the rat uterus in vivo. Following the same approach in our ex vivo studies, we conducted in vivo imaging, frozen sections, and flow cytometry

assays at different time points after transplantation to assess GFP<sup>+</sup> cells.

Frozen section and in vivo imaging results showed that only a small number of GFP<sup>+</sup> cells remained in the uterus of normal rats one day after transplantation of H-eMSC, with no GFP<sup>+</sup> cells detected 3 days or 10 days after the transplantation (Fig. 3A–C). However, in immunosuppressed rats and allogeneic rats, GFP<sup>+</sup> cells were still detectable 10 days post-cell transplantation. These findings suggest that the immune system in normal rats may play a role in eliminating the transplanted human cells, whereas immunosuppression effectively prevents this reaction. In contrast, the transplantation of allogeneic R-eMSC did not trigger a significant immune response and, as a result, remained in the rat uterus for an extended period. Flow cytometry analysis confirmed these findings (Fig. 3D). Transplanted H-eMSC were untraceable after 3 days in rats, whereas they could still be detected 10 days after transplantation in immunosuppressed rats and with allogeneic R-eMSC. These results suggested that, compared with xenotransplantation, allogeneic transplantation may exert long-term therapeutic effects in situ.

#### The therapeutic effect of R-eMSC for IUA rats

MSCs from different tissues have been proven to promote the repair of injured endometrium and improve the pregnancy rate [27–29]. To minimize the potential impact of fluctuations in the rat estrus cycle on our results, we carefully chose the estrus stage as a consistent experimental time point based on analysis of rat vaginal secretions. This decision was motivated by the observation that the rat uterus was thicker during estrus, which we believed would provide a more favorable environment for the experiment (supplement 1A, 1B).

We conducted a comprehensive assessment, evaluating endometrial thickness, the number of glands, the degree of fibrosis, and the number of implanted embryos following the transplantation of R-eMSC. Ten days after eMSC transplantation, we observed a significant restoration of endometrial thickness with R-eMSC treatment ( $814.0 \pm 85.4$ ), comparable to the control ( $877.7 \pm 83.4$ ) and sham-operated ( $869.3 \pm 110.5$ ) groups, and significantly higher than the IUA group ( $521.7 \pm 99$ ). This effect was similar to that observed with autologous eMSC treatment ( $826.3 \pm 123.5$ ). (Fig. 4A, C). The number of endometrial glands also returned to normal levels, consistent with the observed restoration in endometrial thickness following R-eMSC treatment (Fig. 4)A, C. Additionally, we observed a significant reduction in fibrosis, a crucial factor for improving overall tissue health. Our results indicate that both allogeneic R-eMSC transplantation and autologous transplantation significantly reduced the

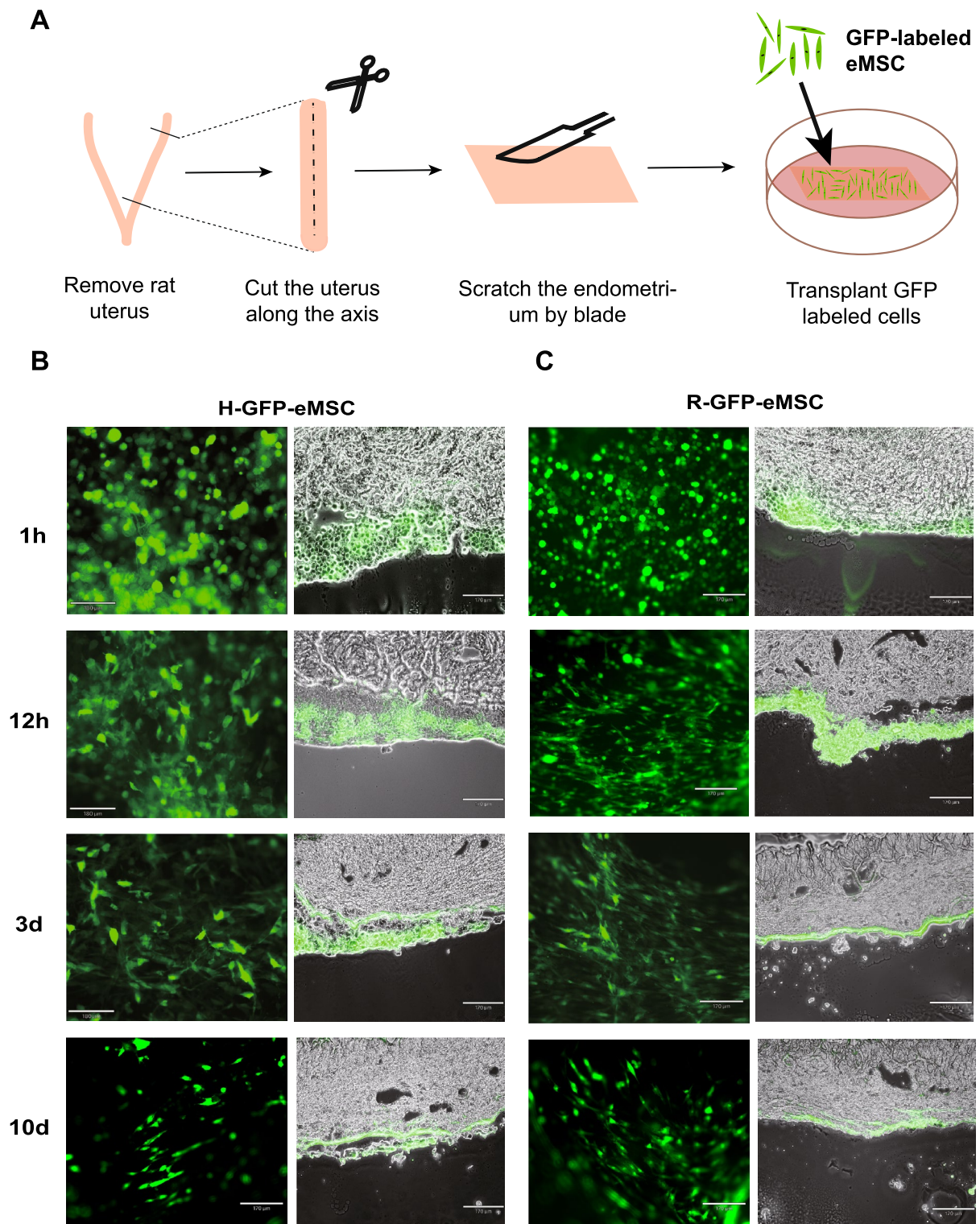


**Fig. 2** Transplant GFP labeled eMSC to endometrium ex vivo. **(A)** Schematic diagram of transplanted H-eMSC and R-eMSC ex vivo. **(B)** Duration after GFP-labeled H-eMSC was transplanted into rat endometrium ex vivo (n=3). Scale bar: 170 μm. **(C)** Duration after GFP-labeled R-eMSC were transplanted into rat endometrium ex vivo (n=3). Scale bar: 170 μm

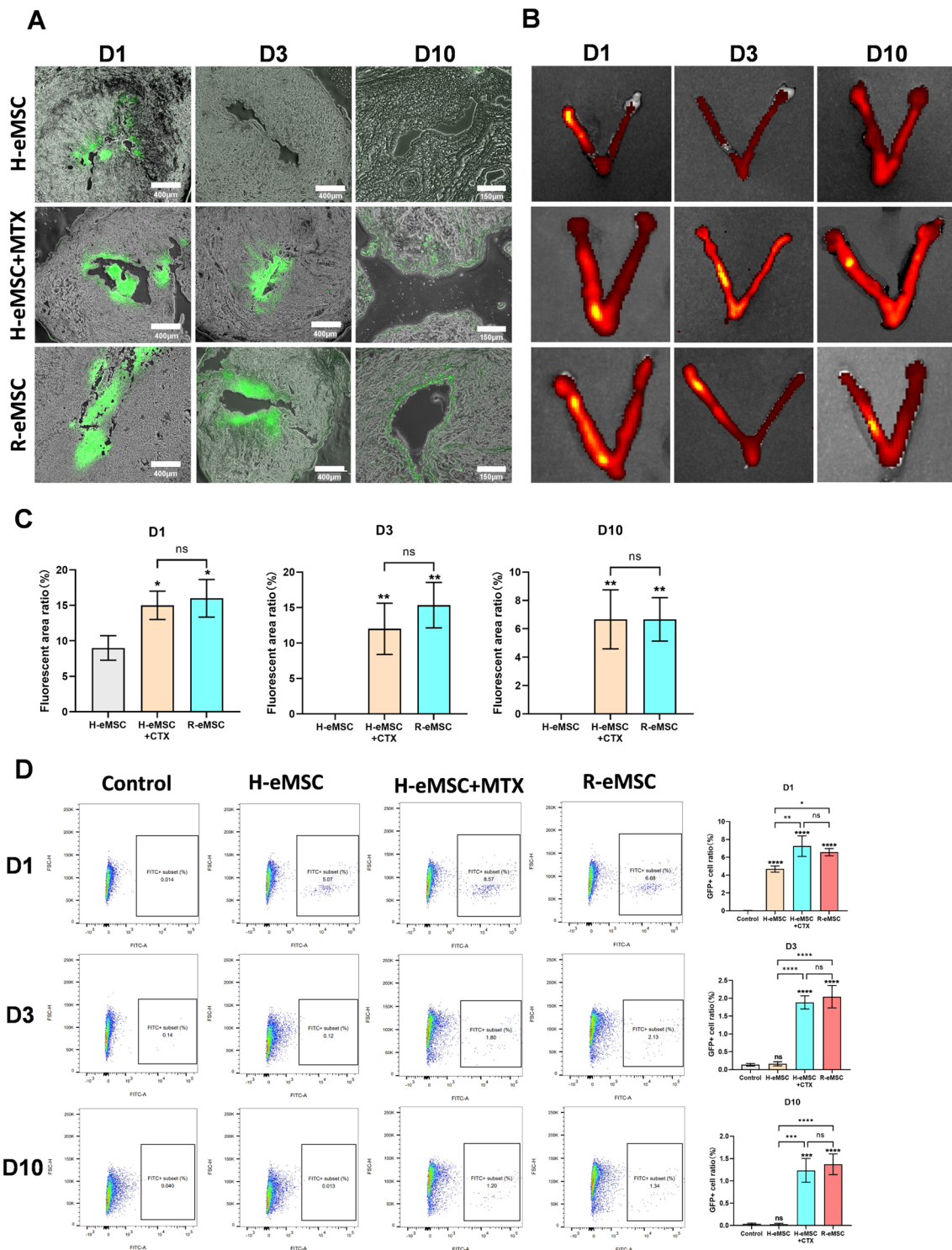


**Fig. 3** Evaluation of H-eMSC and R-eMSC adhesion after in vivo transplantation. **(A)** Frozen section was used to evaluate the retention time of GFP-labeled cells 1, 3, and 10 days after transplantation of H-eMSC, H-eMSC + MTX, and R-eMSC. (D1 and D3 Scale bar: 400  $\mu$ m, D10 Scale bar: 170  $\mu$ m). **(B)** In vivo image was used to evaluate the retention time of GFP-labeled cells 1, 3, and 10 days after transplantation of H-eMSC, H-eMSC + MTX, and R-eMSC. **(C)** Percentage of GFP immunofluorescence positive areas. **(D)** Flow cytometry was used to evaluate the retention time of GFP-labeled cells 1, 3, and 10 days after transplantation of H-eMSC, H-eMSC + MTX, R-eMSC. (Mean  $\pm$  SD, n=3, \*P < 0.05, \*\*P < 0.01, \*\*\*P < 0.001, and \*\*\*\*P < 0.0001)



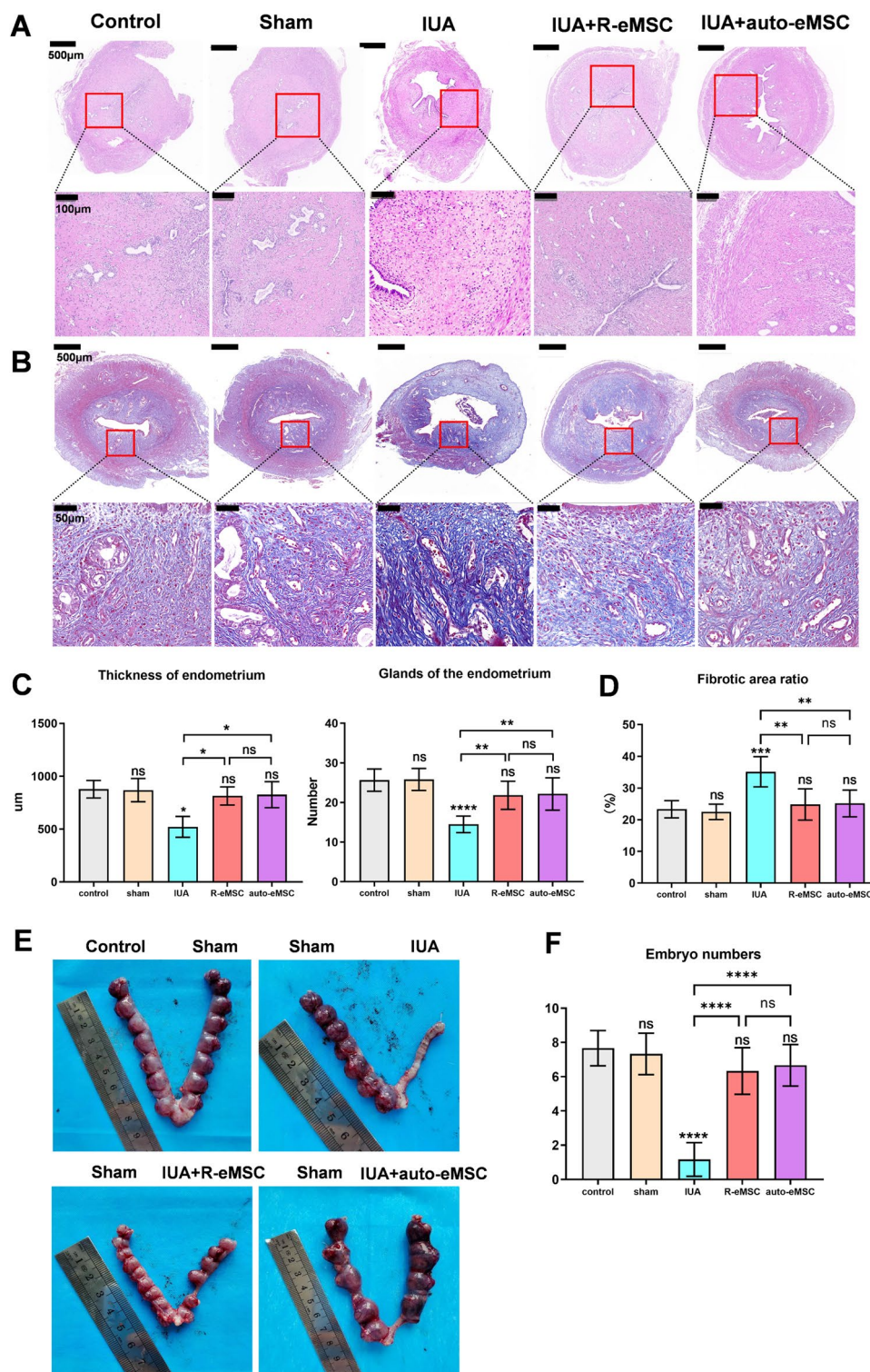


**Fig. 4** Therapeutic effects of R-eMSC on IUA rats. **(A)** H&E staining of rat uteri after different origin eMSC treatments (Scale bars: 500 µm and 100 µm). **(B)** MASSON staining of rat uteri after different origin eMSC treatments (Scale bars: 500 µm and 100 µm). **(C)** Statistical analysis of endometrial thickness and glands of the endometrium under different treatments (n=3). **(D)** Percentage of endometrial fibrosis area (n=3). **(E)** Image of embryo numbers on each side of the uterus after treatment and statistical analysis of the embryo numbers. **(F)** Image of embryo numbers on each side of the uterus after treatment and statistical analysis of the embryo numbers. (Mean ± SD, \*P < 0.05, \*\*P < 0.01, \*\*\*P < 0.001, and \*\*\*\*P < 0.0001)

level of fibrosis in the IUA model, returning it to normal levels (Fig. 4B and D). These results indicate that R-eMSC is beneficial for the regeneration of rat endometrium in the IUA model and significantly reduces the level of endometrial fibrosis in IUA rats.

Furthermore, we performed a fertility test to evaluate the therapeutic effects of allogeneic transplantation on fertility restoration in the model of IUA. Two weeks after the fertility experiment, we examined the implantation efficiency by quantification of the well-developed embryos in different treatment groups. Before conducting the pregnancy experiment, we carried out an autologous cell extraction post-pregnancy test in rats. The results demonstrated that incision and anastomosis of the rat endometrium did not impact the number of embryos after pregnancy in rats. (Supplement 1C). There was no significant difference in the number of implanted embryos between the sham ( $7.67 \pm 0.94$ ) and the control ( $7.33 \pm 1.21$ ) groups, indicating that the sham operation did not affect the pregnancy of the rats (Fig. 4E). The IUA group ( $1.17 \pm 0.98$ ) has less than 20% of embryos implanted. Importantly, after the transplantation of allogeneic R-eMSC ( $6.33 \pm 1.37$ ), the number of embryos was comparable to that of auto-eMSC ( $6.67 \pm 1.21$ ), recovering to 80% of the control group (Fig. 4F). These results suggest that allogeneic transplantation therapy can promote endometrial regeneration and improve fertility.

#### Immune responses after cell transplantation

To investigate the immune responses induced by transplantation of cells of H-eMSC and R-eMSC, we quantified the ratio of lymphocytes (CD45-positive) and macrophages (CD68-positive) in rat endometrial tissue Sections 3 days post-transplantation (Fig. 5A, B). Our findings revealed significant immune cell infiltration after the transplantation of H-eMSC, whereas the response was notably milder with R-eMSC (Fig. 5C). This suggests that the immune response to allogeneic MSCs is less aggressive compared to xenogeneic MSCs, which could contribute to the observed long-term engraftment and therapeutic benefits. Furthermore, we have included a group of rats that underwent immunosuppression following the transplantation of H-eMSC. Importantly, pre-treatment with immunosuppressants effectively prevented immune cell infiltration in the context of xenotransplantation, highlighting the importance of immune modulation in the success of MSC transplantation. These results underscore the differential immune responses to allogeneic versus xenogeneic MSCs and provide a mechanistic explanation for the observed therapeutic outcomes.

Taken together, our study demonstrates that allogeneic transplantation of R-eMSC in the IUA rat model can

engraft and exert long-term therapeutic effects to restore endometrium tissue injury and fertility capability.

#### Discussion

Cell transplantation therapy is considered the most promising treatment for moderate and severe IUA. Human MSCs derived from different sources, such as bone marrow, adipose tissue, umbilical cord, and menstrual blood, are found to repair endometrial injury and recover fertility ability in various animal models. However, most of the xenotransplantation research does not involve immune suppression, and the therapeutic effects are considered short-term through paracrine secretions. More importantly, these xenotransplantation settings are not able to recapitulate what happens in human clinical trials, which involve allogenic or autologous cell transplantation. Here, we established an allogenic transplantation model in rats to study the engraftment and long-term therapeutic effects of eMSC on IUA. We also compared the engraftment duration of allogenic transplantation to routinely used xenotransplantation models, as well as the underlying molecular mechanisms.

Based on our results, we found that H-eMSC and R-eMSC can quickly adhere to the rat endometrium tissue and attach to it for more than 10 days *ex vivo*. However, once it happens *in vivo*, H-eMSC can only stay in normal SD rats (without immune suppression) for less than 3 days, and then be cleared by the immune rejection from the host. When the rat's immunity is suppressed by MTX, H-eMSC can persist in the uterine for 10 days. Importantly, in the allogeneic model, R-eMSC can engraft in the rat endometrium for much longer. They are detectable 10 days after transplantation, as evidenced by flow cytometry, *in vivo* imaging, and staining. After the transplantation of H-eMSC, infiltration of immune cells was significantly higher compared to H-eMSC+MTX and allogeneic R-eMSC, indicating that allogeneic H-eMSC may activate the host immune response to eliminate the transplanted cells. This long-term allograft indicates that, in the pre-clinical animal studies, allogeneic transplantation studies might be more predictive in terms of outcomes, and more suitable to dissect the mechanisms of action (MOA) of cell transplantation therapy.

In the clinic, IUA patients seeking stem cell-based therapy are more likely to be infertile and suffer from several complications after surgical treatment. In the clinical trials, IUA patients expect to receive allogenic/ or autogenous transplantation therapy. Most importantly, the patients would expect the therapeutic effects to be long-lasting and effective. Stem cells, especially eMSC that are derived from the injured tissue, are supposed to engraft and actively participate in tissue repair and regeneration. Our study has established

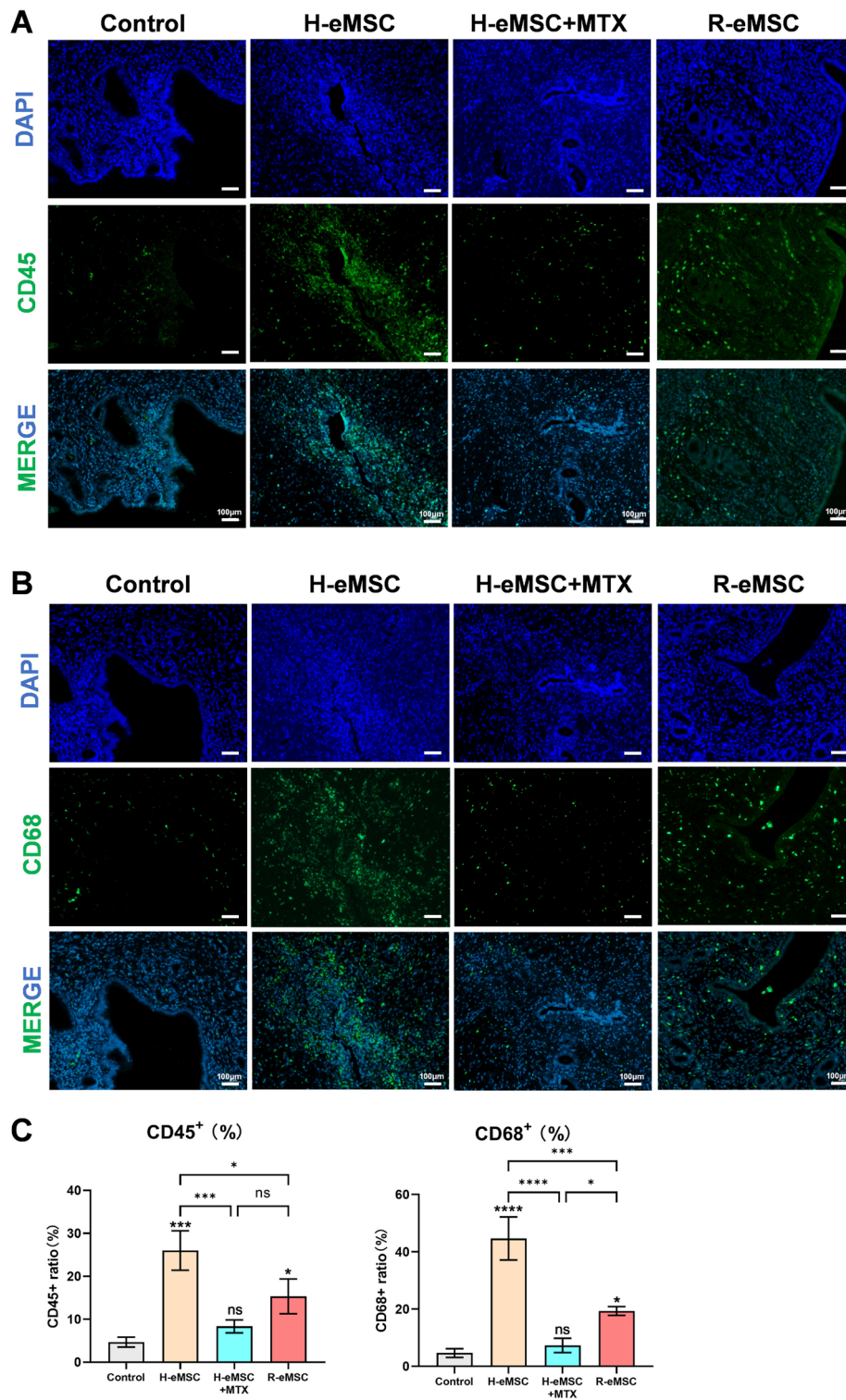


**Fig. 5** Expression of immune cells after cell transplantation. **(A)** Immunofluorescence images of CD45-positive cells between different groups 3 days after transplantation (Scale bar: 100  $\mu$ m). **(B)** Immunofluorescence images of CD68-positive cells between different groups 3 days after transplantation (Scale bar: 100  $\mu$ m). **(C)** Percentages of CD45 and CD68 positive cells. (Mean  $\pm$  SD, n = 3, \*P < 0.05, \*\*P < 0.01, \*\*\*P < 0.001, and \*\*\*\*P < 0.0001)

a good model to set the foundation to investigate the MOA of eMSC in the injured tissue. However, more detailed work needs to be done to further elucidate the MOA, including purification and characterization of the engrafted cells, and identification of key factors that determine the therapeutic effects of the engrafted cells. In addition, allogeneic transplantation animal models should also be established to recapitulate the therapeutic process in human clinical trials.

## Conclusions

The present study demonstrates that allogeneic transplantation of R-eMSC can engraft into rat endometrium for the long term and promote the repair of IUA. Allogeneic transplantation therapy contributes to a thicker endometrium, more glands in an injured endometrium, and restore fertility capability in an IUA rat model. We also investigated widely used xenograft systems and observed that only a small fraction of H-eMSCs could be implanted in the rat endometrium. Xenogeneic transplantation was subsequently activated the local immune system and cleared by the rat immune system within 3 days post-transplantation. In contrast, the immunosuppressed rats retained H-eMSCs in the uterus for up to 10 days, a colonization period similar to that of allogeneic cell transplantation, indicating that prolonged colonization is more favorable for tissue recovery. Our study provides a system to study the precise mechanism of how stem cell grafting improves endometrial regeneration.

## Abbreviations

|        |                                                  |
|--------|--------------------------------------------------|
| IUA    | Intrauterine adhesion                            |
| GFP    | Green fluorescence proteins                      |
| PBS    | Phosphate-buffered saline                        |
| DMEM   | Dulbecco's modified Eagle's medium               |
| FBS    | Fetal bovine serum                               |
| MSCs   | Mesenchymal stem cells                           |
| eMSC   | Endometrial mesenchymal stem cells               |
| H-eMSC | Human endometrium-derived mesenchymal stem cells |
| R-eMSC | Rat endometrium-derived mesenchymal stem cells   |
| H&E    | Hematoxylin and Eosin                            |
| MTX    | Methotrexate                                     |
| MOA    | Mechanisms of action                             |

## Acknowledgements

Not applicable

## Author contributions

KC: Conception and design, provision of study material, collection and assembly of data, final approval of the manuscript. Yy G: Provision of study material or patients, collection and assembly of data, data analysis and interpretation. Nn X: Conception and design, Collection and/or assembly of data, data analysis, and interpretation. YS L: Collection of the endometrium samples, collection, and assembly of data. Hr W: Acquisition, analysis of the work, final approval of the manuscript. H M: Analysis of the work, collection, and assembly of data. Sx Z: Conception and design, final approval of the manuscript. FF: Conception and design, data analysis and interpretation, manuscript writing, and final approval of the manuscript.

## Funding

This work was supported by grants from the National Key R&D Programme of China (2022YFA0806301 to F.F.), Grant No. 32070830 and Grant No. 81971339 from the National Natural Science Foundation of China, and the University of Science and Technology of China WK9110000141, and YD9100002007.

## Availability of data and material

The datasets used and/or analyzed during the current study are available from the corresponding author upon reasonable request.

## Declarations

### Ethics approval and consent to participate

H-eMSC were obtained from the First Affiliated Hospital of USTC, Division of Life Sciences and Medicine, University of Science and Technology of China, Hefei, Anhui, China. Collection of the H-eMSC was approved by the Institutional Animal Care and Use Committee at the First Affiliated Hospital of USTC (code no. 2023KY300, Title: Therapeutic effects of mesenchymal stem cell for intrauterine adhesion. Date of approval: 14 Sep 2023), and all the patients signed informed consent before participating in the study. All animal experiments were conducted in accordance with the Guide for the Care and Use of Animals for Research Purposes. All the procedures were approved by the Institutional Animal Care and Use Committee at the First Affiliated Hospital of USTC (code no. 2022-N(A)-119, Title: Regulatory network of Wnt/ $\beta$ -catenin signaling pathway in menstrual blood stem cells repairing thin endometrial fertility. Date of approval: 9 May 2023).

### Consent for publication

All authors gave consent for publication.

### Competing interests

The authors declare that they have no competing interests.

### Author details

<sup>1</sup>Reproductive Medicine Center and Department of Obstetrics and Gynecology, The First Affiliated Hospital of USTC, Division of Life Sciences and Medicine, University of Science and Technology of China, Hefei 230001, Anhui, China. <sup>2</sup>Anhui Tianlun Infertility Specialist Hospital, Hefei, China. <sup>3</sup>The First Affiliated Hospital of USTC, Division of Life Sciences and Medicine, University of Science and Technology of China, Hefei 230001, Anhui, China. <sup>4</sup>CodeR Therapeutics, Ltd., Hefei 230027, Anhui, China.

Received: 19 July 2024 Accepted: 7 December 2024

Published online: 23 December 2024

## References

- Critchley HOD, Maybin JA, Armstrong GM, et al. Physiology of the endometrium and regulation of menstruation. *Physiol Rev*. 2020;100(3):1149–79.
- Santamaria X, Isaacson K, Simón C. Asherman's syndrome: it may not be all our fault. *Hum Reprod*. 2018;33(8):1374–80.
- Hooker A, Fraenk D, Brölmann H, et al. Prevalence of intrauterine adhesions after termination of pregnancy: a systematic review. *Europ J Contr Reprod Health Care Off J Europ Soc Contr*. 2016;21(4):329–35.
- Chen MJ, Yang JH, Peng FH, et al. Extended estrogen administration for women with thin endometrium in frozen-thawed in-vitro fertilization programs. *J Assist Reprod Genet*. 2006;23(7–8):337–42.
- Momeni M, Rahbar MH, Kovanci E. A meta-analysis of the relationship between endometrial thickness and outcome of in vitro fertilization cycles. *J Human Reprod Sci*. 2011;4(3):130–7.
- Yuan X, Saravelos SH, Wang Q, et al. Endometrial thickness as a predictor of pregnancy outcomes in 10787 fresh IVF-ICSI cycles. *Reprod Biomed Online*. 2016;33(2):197–205.
- Hanstedde MM, van der Meij E, Goedemans L, et al. Results of centralized Asherman surgery, 2003–2013. *Fertil Steril*. 2015;104(6):1561–8.e1561.
- Roy KK, Negi N, Subbaiah M, et al. Effectiveness of estrogen in the prevention of intrauterine adhesions after hysteroscopic septal resection: a prospective, randomized study. *J Obstet Gynaecol Res*. 2014;40(4):1085–8.

9. Eftekhari M, Neghab N, Naghshineh E, et al. Can autologous platelet rich plasma expand endometrial thickness and improve pregnancy rate during frozen-thawed embryo transfer cycle? A randomized clinical trial. *Taiwan J Obstet Gynecol*. 2018;57(6):810–3.
10. Lebovitz O, Orvieto R. Treating patients with “thin” endometrium - an ongoing challenge. *Gynecol Endocrinol*. 2014;30(6):409–14.
11. Jing Z, Qiong Z, Yonggang W, et al. Rat bone marrow mesenchymal stem cells improve regeneration of thin endometrium in rat. *Fertil Steril*. 2014;101(2):587–94.
12. Gao L, Huang Z, Lin H, et al. Bone marrow mesenchymal stem cells (BMSCs) restore functional endometrium in the rat model for severe Asherman syndrome. *Reprod Sci*. 2019;26(3):436–44.
13. Santamaria X, Cabanillas S, Cervelló I, et al. Autologous cell therapy with CD133+ bone marrow-derived stem cells for refractory Asherman's syndrome and endometrial atrophy: a pilot cohort study. *Hum Reprod*. 2016;31(5):1087–96.
14. Zheng S, Gao Y, Chen K, et al. A robust and highly efficient approach for isolation of mesenchymal stem cells from wharton's jelly for tissue repair. *Cell Transplant*. 2022;31:9636897221084354.
15. Ding DC, Shyu WC, Lin SZ. Mesenchymal stem cells. *Cell Transplant*. 2011;20(1):5–14.
16. Minter D, Marra KG, Rubin JP. Adipose-derived mesenchymal stem cells: biology and potential applications. *Adv Biochem Eng Biotechnol*. 2013;129:59–71.
17. Chen L, Zhang C, Chen L, et al. Human menstrual blood-derived stem cells ameliorate liver fibrosis in mice by targeting hepatic stellate cells via paracrine mediators. *Stem Cells Transl Med*. 2017;6(1):272–84.
18. Chen K, Wang H, Zhao X, et al. A novel method to repair thin endometrium and restore fertility based on menstruation-derived stem cell. *Reprod Sci (Thous Oaks Calif)*. 2024;31(6):1662–73.
19. Lopes L, Setia O, Aurshina A, et al. Stem cell therapy for diabetic foot ulcers: a review of preclinical and clinical research. *Stem Cell Res Ther*. 2018;9(1):188.
20. Liu XY, Yang LP, Zhao L. Stem cell therapy for Alzheimer's disease. *World J Stem Cells*. 2020;12(8):787–802.
21. Bagno L, Hatzistergos KE, Balkan W, et al. Mesenchymal stem cell-based therapy for cardiovascular disease: progress and challenges. *Mol Ther*. 2018;26(7):1610–23.
22. Wang H, Chen K, Zong L, et al. MALAT1/miR-7-5p/TCF4 axis regulating menstrual blood mesenchymal stem cells improve thin endometrium fertility by the wnt signaling pathway. *Cell Transplant*. 2024;33:9636897241259552.
23. Liu H, Zhang X, Zhang M, et al. Mesenchymal stem cell derived exosomes repair uterine injury by targeting transforming growth factor- $\beta$  signaling. *ACS Nano*. 2024;18(4):3509–19.
24. Song M, Ma L, Zhu Y, et al. Umbilical cord mesenchymal stem cell-derived exosomes inhibits fibrosis in human endometrial stromal cells via miR-140-3p/FOXP1/Smad axis. *Sci Rep*. 2024;14(1):8321.
25. Stolzing A, Scutt A. Age-related impairment of mesenchymal progenitor cell function. *Aging Cell*. 2006;5(3):213–24.
26. Ajayi AF, Akhigbe RE. Staging of the estrous cycle and induction of estrus in experimental rodents: an update. *Fertility Res Pract*. 2020;6:5.
27. Chang QY, Zhang SW, Li PP, et al. Safety of menstrual blood-derived stromal cell transplantation in treatment of intrauterine adhesion. *World J Stem Cells*. 2020;12(5):368–80.
28. Yang H, Wu S, Feng R, et al. Vitamin C plus hydrogel facilitates bone marrow stromal cell-mediated endometrium regeneration in rats. *Stem Cell Res Ther*. 2017;8:267. <https://doi.org/10.1186/s13287-017-0718-8>.
29. Yu J, Zhang W, Huang J, et al. Management of intrauterine adhesions using human amniotic mesenchymal stromal cells to promote endometrial regeneration and repair through Notch signalling. *J Cell Mol Med*. 2021;25(23):11002–15.

## Publisher's Note

Springer Nature remains neutral with regard to jurisdictional claims in published maps and institutional affiliations.